Electrical Power and Energy Systems 43 (2012) 1376–1382

Contents lists available at SciVerse ScienceDirect

Electrical Power and Energy Systems

journal homepage: www.elsevier.com/locate/ijepes

A novel method for adaptive distance protection of transmission line connected to wind farms

Hadi Sadeghi

Department of Electrical Engineering, Amirkabir University of Technology, Tehran, Iran

ARTICLE INFO

Article history:
Received 8 July 2010
Received in revised form 17 June 2012
Accepted 26 June 2012
Available online 31 July 2012

Keywords:
Adaptive protection
Digital protection
Distance relaying
Wind farm

ABSTRACT

Wind speed variations results in wind farm voltage, frequency and power output fluctuations. Therefore, protection of lines connecting such a farm to the grid is very important and an adaptive system for distance protection of such a line is necessary. In this paper, an adaptive unit which adjusts the relay trip characteristic using local information has been designed for distance relay using artificial neural networks. In this case, in order to prevent wrong operation of relay, changing in wind farm conditions, the set points of different zones of distance relay has to be changed simultaneously. The results obtained from proposed method are verified by computer simulation.

1. Introduction

Wind farms are increasingly integrated to the grids at different levels of voltage across the world. The share of such farms in a power system is also rising day by day. The problem that arises in integrating such farms is primarily due to variable wind speed. The speed variation results in fluctuating output power. The output power of a generating unit has a nonlinear relationship with the wind speed, and when the speed is beyond the limits, the farm cannot contribute to the grid [1]. In addition, due to under/over voltage conditions, a group of turbines may trip while others may remain in operation. Obviously, the transmission system that connects such farms will be exposed to such a continuously changing environment. In most papers, topics related to protection of wind farms have discussed about over-current relay setting in distribution systems and adaptive schemes are proposed for distribution systems connected with wind generators [2,3]. The protection of transmission line connected to wind farms is discussed in [4]. Distance relays are commonly used for line protection either as primary or backup. Their digital version has advantages of better monitoring, communication, and adaptation to system condition. Adaptive forms of distance relays are proposed to overcome associated problems in real time, which ultimately increase the overall reliability index of the protection scheme [5–13]. In distance protection, to coordinate high fault resistance with ground faults, quadrilateral characteristic is preferred. In a fixed setting approach, the boundary of the relay characteristic is predefined based on overall system study. With an adaptive feature in a distance relay, the boundary is set online in accordance with the prevailing condition. In [6], the trip boundary is set adaptively that assumes that through SCADA or PMU voltages and line flows of all parts of the system are available. The module of adaptive relay using the swiveling quadrilateral characteristics that the angle of swivel is computed using residual current where the fault area is assumed to be fixed, is proposed in [7]. The proposed scheme in [8] is based on neural network using real and reactive power at the relay location as the input vector. Such an approach provides an approximate solution and the neural network is not valid for another system.

In adaptive scheme which is proposed in this paper, the ratio of local current and voltage and instant information of wind farm has been used for adaptive protection. The proposed approach is simple to implement and provides accurate settings for such a system. Results are provided for a line-to-ground fault and the concept can be extended to other types of faults. The trip characteristic of a relay is decided from detailed off-line study of the system. In an adaptive form, the trip boundary should be changed as the system condition change. In [6], the mathematical formulation is outlined for generating trip boundary in the case of line-to-ground fault. The trip boundary considered here is of quadrilateral characteristic on an impedance plane obtained by varying fault location and fault resistance within their limits.

2. Ideal trip characteristic for distance relay

In a wind farm, a number of units are connected in parallel to harness bulk amounts of electric power for a grid. When such a

E-mail address: hsadeghi.hadi@gmail.com

0142-0615/$ - see front matter © 2012 Elsevier Ltd. All rights reserved.
http://dx.doi.org/10.1016/j.ijepes.2012.06.072

potentially high level of generation is available at a remote place, transmission systems are hooked up for efficient power management. As the generation at a wind farm fluctuates, the connecting line will see varying degrees of transmitted power through a day. The fluctuations of voltage and frequency in the system depend on the proportionate strength of the farm. To see the effects of wind farm operating conditions on trip characteristic, a 400 kV, 60 Hz power system is studied later [6].

A schematic of a typical wind farm connection is shown in Fig. 1. In this figure, the wind farm supplies power to the grid through the transmission network that is protected by a distance relay. The line diagram of the power system for phase-A-to-ground fault in the line is shown in Fig. 2. The considered distance relay is positioned at W and the normal power flow direction in the system is from W to P (wind farm to grid) as marked in the figure. In this analysis, the wind farm and the grid are considered with their equivalent simplified models and shunt capacitance is not considered for the line.

The system parameters are presented in Table 1.

The pre-fault voltage relation of the equivalent sources is defined as

$$E_{AP} = \rho e^{-j\delta} E_{AW} \quad (1)$$

The pre-fault current can be written as

$$I_{WP} = (E_{AW} - E_{AP})/Z_1 \quad (2)$$

where Z_1 is the positive sequence impedance of the system and can be obtained as

$$Z_1 = Z_{1SW} + Z_{1L} + Z_{1SP} \quad (3)$$

From voltage and current relations in (1) and (2), the following can be written

$$\rho e^{-j\delta} = 1 - (I_{WP}/E_{AW})Z_1 \quad (4)$$

If system conditions ($\rho, \delta, Z_{SP}, Z_{SW}$) are fixed and R_F and fault location varied, four boundary lines, defined below, are obtained by computer simulation (Fig. 3).

Line I: solid faults at different points of line.
Line II: faults at relay-reach end (90% of line length) with different fault resistance up to 50 Ω.
Line III: faults at different points with a 50 Ω fault resistance.
Line IV: faults at the relaying point with different fault resistance up to 50 Ω.

These four lines and included area define ideal trip region of relay under the prevailing system conditions.

In [14], it is shown that variation of two parameters as wind farm local information affects on seen impedance by the distance relay and ideal trip characteristic. These parameters are equivalent impedance of the wind farm (Z_{1SW}) and the ratio of current and voltage in relay point (I_{WP}/E_{AW}).

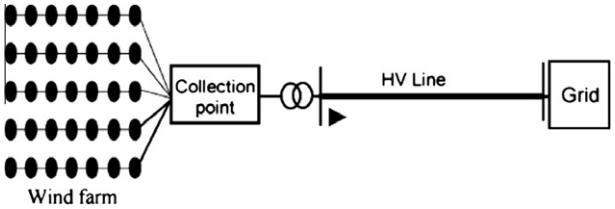

Fig. 1. Interconnection of wind farm to the grid [14].

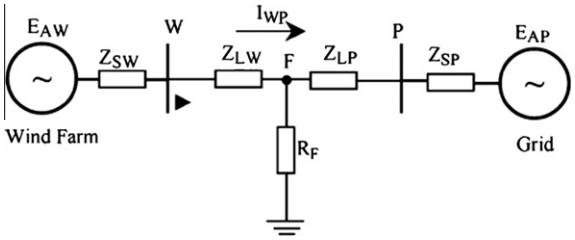

Fig. 2. Line diagram for phase A-to-ground fault [14].

Table 1
Values of different parameters of studied system.

	Z_{SW} (Ω)	Z_{SP} (Ω)	Z_L (Ω)
Zero sequence	30∠85°	1.5∠85°	87.35∠83°
Positive sequence	20∠85°	1∠85°	28.75∠86°

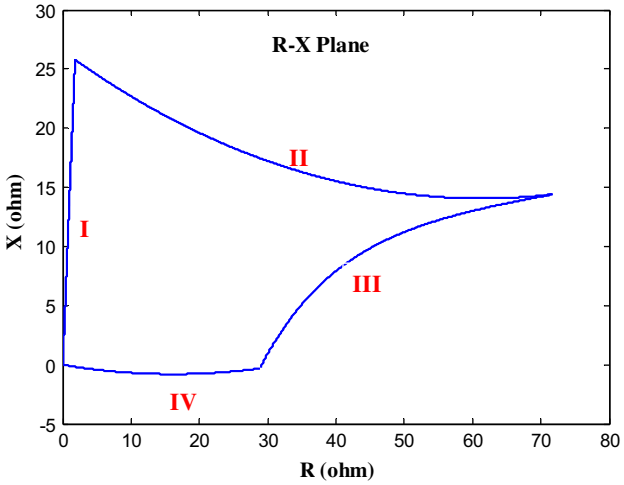

Fig. 3. Ideal trip characteristic for $Z_{1SW} = 20\angle 85°$, $Z_{0SW} = 30\angle 85°$, $\rho = 0.95$, $\delta = 20$.

3. Proposed adaptive protection scheme

To prevent mal-operation of distance relay, it is necessary that relay trip decision can change by variations of wind farm conditions. In fact, for a point in firs zone of relay (90% of line length), impedance value seen by relay must be included inside of trip characteristic. Thus, the four lines which determines relay trip boundaries must be varied with wind farm conditions (the amount of I_{WP}/E_{AW} and equivalent impedance of the wind farm). Therefore, how to make a distance relay operate sensitively as these conditions vary is the main problem that must be solved. To solve this problem, two different approaches can be proposed:

(1) Firstly, setting patterns under all possible system conditions can be calculated off-line and stored in a data table for using during fault. Alternatively, only one set of setting parameters are calculated on-line and they are renewed from time to time as the system conditions change. When a fault occurs the relay will operate with the latest setting parameters, an optimal trip boundary [6].

This method is faster in on-line processing due to less computation. However, a large amount of computer memory would be needed to cover all the possible conditions. Also, the nonlinear boundaries will make it more complex.

Relay setting is the other important problem. Mho relay is the simplest kind of relay can be used. In this case the ideal trip characteristic which is a quadrilateral shape with nonlinear boundaries, are surrounded in circle of mho characteristic. However, since the included area of ideal characteristic is very less than its environment circle surface, particularly for large amount of Z_{1SW}, and different zones of relay may intervene together, using of mho relay does not seem reasonable. Also, this relay may trouble in over-reach or under-reach problem in presence of fault resistance and thus, quadrilateral relay should be used instead of mho relay.

Ideal trip characteristic can be fitted in a real quadrilateral distance relay characteristic in an optimized manner as shown in Fig. 4.

But this work has the problem of intervention of shaded area with the second zone of relay. If the shaded area can be deleted, the worry of invention of zone-1 and zone-2 will be obviated. For this purpose, described approach in the following will be preceded to obtain zone-1 trip decision.

(2) Adaptive scheme: the computation of the adaptive setting scheme consists of two parts:
(I) The computation of the setting boundaries.
(II) The calculations performed during a fault.

This scheme which has been carefully designed, minimize calculation of both parts while maintaining high reach accuracy. In this scheme, a number of straight line segments are used to approximate the curved boundaries in Fig. 3. The number of the straight lines is determined by the precision required and processing capacity of the processor. Here, three straight lines 2, 4, 6 are used for line II, two 8, 10 for line III, two 12, 13 for line IV and line 1 for line I. This approximate model is shown in Fig. 5.

Each line divides the R–X plane into two region and we suppose that a "line output" is positive if the measured impedance falls on one side of the line and negative on the other side. The positive or zero value of line output is assumed comparable with logical "1" and negative value with "0". If the ideal trip region remained a convex shape these linear outputs and some "AND" operations could well determine a trip decision during fault. However, since different system conditions will result in different curved boundaries, the decision region may be non-convex. Hence mere logical "AND" operations of the linear outputs cannot be relied upon for the trip decisions. For this reason, additional lines are used to divide the decision region into several sub-regions. These lines are shown with numbers 5, 7, 9, 11 and 13 in Fig. 5. The linear outputs for straight lines 1–13 in Fig. 5 correspond to signals L1–L13 in Fig. 6.

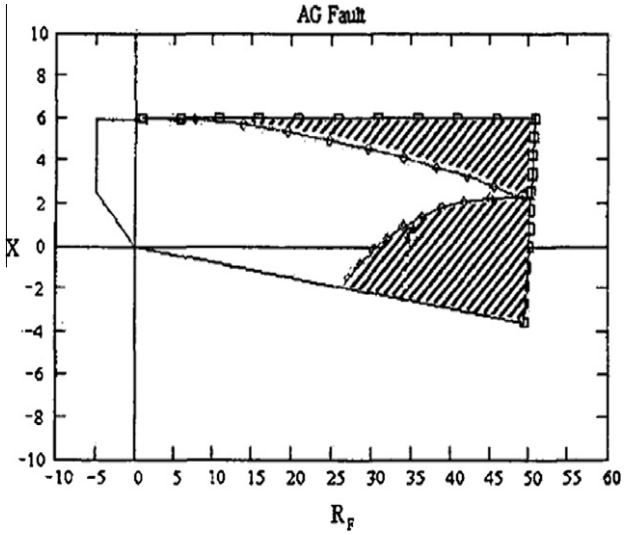

Fig. 4. Optimized trip characteristic for distance relay and ideal trip characteristic.

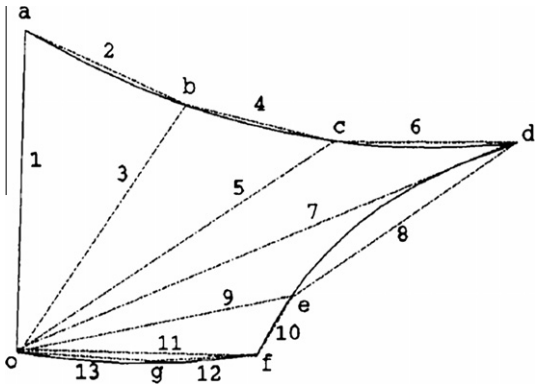

Fig. 5. Adaptive setting characteristic and topological trip-decision logic [6].

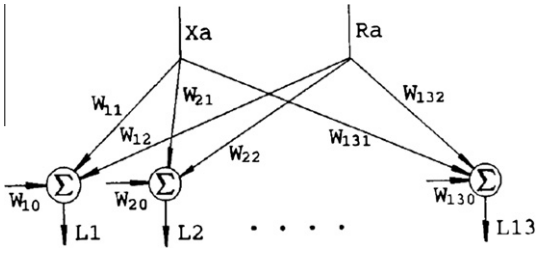

Fig. 6. Calculation architecture in adaptive setting [6].

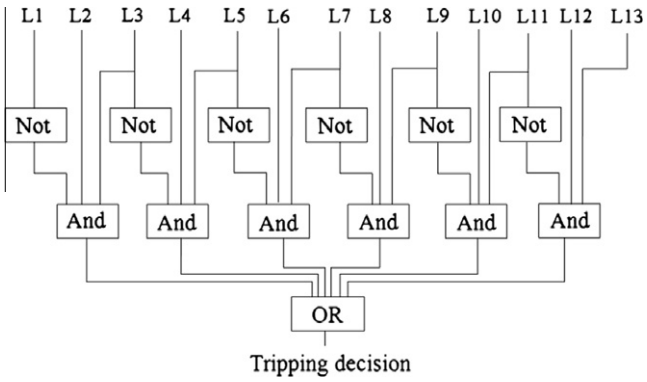

Fig. 7. Trip decision logic circuit [6].

Now, a combination of logical "AND" and "OR" operations of these signals can be used to obtain reliable trip decision. Each linear output is connected to the measured reactance and resistance through two weights. A bias weight is also connected to the linear output. For example, for L1 we have W_{11} and W_{12} and also bias weight of W_{10}. The output value is defined by

$$L_1 = W_{11}X_A + W_{12}R_A + W_{10} \tag{5}$$

Positive and negative values of the output determine the two sides of the line. A critical thresholding condition occurs when the linear output equals zero:

$$W_{11}X_A + W_{12}R_A + W_{10} = 0 \tag{6}$$

Therefore:

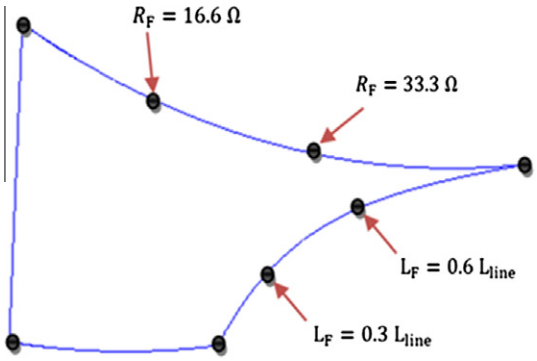

Fig. 8. Position of selected points for polygonal trip characteristics corners.

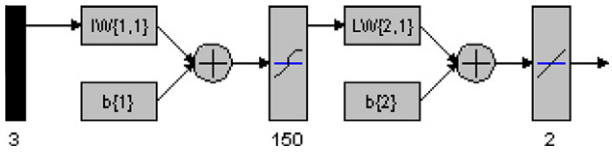

Fig. 9. 3rd Neural network diagram.

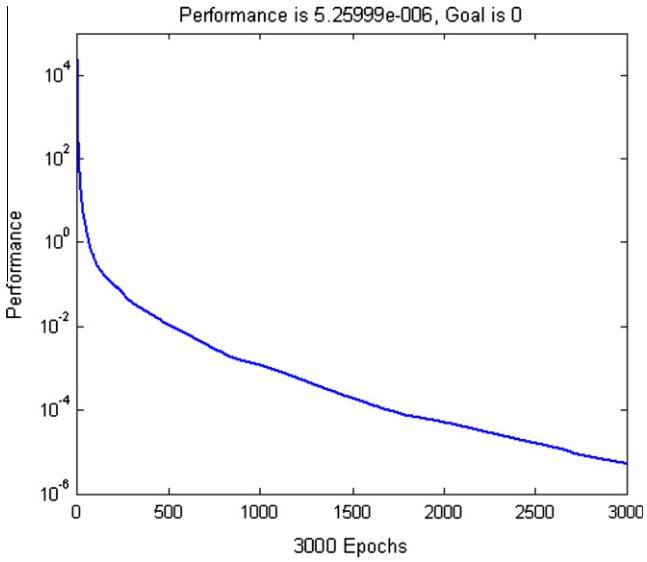

Fig. 10. Performance function of 3rd network.

$$X_A = (-W_{12}/W_{11})R_A + (-W_{10}/W_{11}) \quad (7)$$

It is obvious that the above equation expresses a straight line having slope and intercept given by $(-W_{12}/W_{11})$ and $(-W_{10}/W_{11})$ respectively and, therefore, the three weights. W_{10}, W_{11} and W_{12}, determine the slope, intercept, and side of separating line.

For example, in the case of line "1" in Fig. 5 the intercept is zero and the slope can be determined by resistance and reactance at "a" only. Supposing the linear output is positive on the left side of the line, and selecting $W_{11} = \pm 1$ (to minimize on-line calculation during faults), the three weights are:

$$\begin{aligned} W_{10} &= 0 \\ W_{11} &= 1 \\ W_{12} &= -X_A(a)/R_A(a) \end{aligned} \quad (8)$$

A similar method is used to obtain weights for L3, L5, L7, L9, L11 and L13. However, it is only slightly more complex to determine the weights for L2, L4, L6, L8, L10 and L12. Taking L2 as an example we have:

$$L_2 = W_{21}X_A + W_{22}R_A + W_{20} = 0 \quad (9)$$

Table 2
The values of resistance and reactance of 3rd point for different condition of system.

	$Z_{1SW} = 20\angle 85°$	$Z_{1SW} = 40\angle 85°$	$Z_{1SW} = 60\angle 85°$	$Z_{1SW} = 80\angle 85°$	$Z_{1SW} = 20\angle 85°$
$\rho = 0.9$, $\delta = 3°$	(94.59, 43.83)	(124.57, 48.74)	(154.07, 53.65)	(183.33, 58.56)	(212.45, 63.47)
$\rho = 0.9$, $\delta = 6°$	(87.30, 36.77)	(115.38, 39.83)	(143.04, 42.92)	(170.47, 46.03)	(197.78, 49.14)
$\rho = 0.9$, $\delta = 9°$	(80.75, 31.35)	(107.10, 32.87)	(133.07, 34.46)	(158.83, 36.07)	(184.48, 37.69)
$\rho = 0.9$, $\delta = 12°$	(74.89, 27.12)	(99.66, 27.36)	(124.08, 27.68)	(148.32, 28.04)	(172.45, 28.42)
$\rho = 0.9$, $\delta = 15°$	(69.66, 23.78)	(92.98, 22.93)	(115.98, 22.19)	(138.83, 21.49)	(161.57, 20.83)
$\rho = 0.9$, $\delta = 18°$	(64.98, 21.10)	(86.97, 19.33)	(108.67, 17.68)	(130.24, 16.09)	(151.71, 14.54)
$\rho = 0.9$, $\delta = 21°$	(60.78, 18.93)	(81.54, 16.37)	(102.06, 13.95)	(122.44, 11.59)	(142.75, 9.27)
$\rho = 0.9$, $\delta = 24°$	(57.00, 17.15)	(76.63, 13.92)	(96.05, 10.82)	(115.35, 7.80)	(134.58, 4.82)
$\rho = 0.9$, $\delta = 27°$	(53.58, 15.68)	(72.16, 11.85)	(90.56, 8.18)	(108.86, 4.58)	(127.10, 1.02)
$\rho = 0.9$, $\delta = 30°$	(50.46, 14.44)	(68.08, 10.11)	(85.54, 5.93)	(102.91, 1.82)	(120.22, −2.23)
$\rho = 1.0$, $\delta = 3°$	(108.29, 23.94)	(141.87, 24.13)	(174.92, 24.40)	(207.71, 24.71)	(240.34, 25.04)
$\rho = 1.0$, $\delta = 6°$	(97.44, 19.72)	(128.49, 18.55)	(159.05, 17.50)	(189.37, 16.50)	(219.54, 15.53)
$\rho = 1.0$, $\delta = 9°$	(88.42, 16.66)	(117.22, 14.38)	(145.60, 12.25)	(173.74, 10.19)	(201.75, 8.16)
$\rho = 1.0$, $\delta = 12°$	(80.80, 14.38)	(107.62, 11.19)	(134.05, 8.17)	(160.28, 5.22)	(186.38, 2.32)
$\rho = 1.0$, $\delta = 15°$	(74.30, 12.65)	(99.34, 8.70)	(124.04, 4.93)	(148.55, 1.25)	(172.96, −2.37)
$\rho = 1.0$, $\delta = 18°$	(68.67, 11.29)	(92.12, 6.71)	(115.26, 2.32)	(138.25, −1.97)	(161.14, −6.21)
$\rho = 1.0$, $\delta = 21°$	(63.76, 10.23)	(85.77, 5.11)	(107.51, 10.18)	(129.12, −4.63)	(150.65, −9.40)
$\rho = 1.0$, $\delta = 24°$	(59.43, 9.38)	(80.13, 3.80)	(100.61, −1.57)	(120.97, −6.85)	(141.25, −12.07)
$\rho = 1.0$, $\delta = 27°$	(55.58, 8.69)	(75.10, 2.72)	(94.42, −3.05)	(113.64, −8.73)	(132.79, −14.34)
$\rho = 1.0$, $\delta = 30°$	(52.13, 8.13)	(70.56, 1.81)	(88.83, −4.30)	(107.01, −10.32)	(125.12, −16.28)
$\rho = 1.1$, $\delta = 3°$	(112.74, 0.16)	(148.44, −5.00)	(183.51, −10.01)	(218.26, −14.95)	(252.83, −19.86)
$\rho = 1.1$, $\delta = 6°$	(100.54, 0.48)	(133.28, −5.37)	(165.46, −11.02)	(197.37, −16.56)	(229.10, −22.04)
$\rho = 1.1$, $\delta = 9°$	(90.64, 0.76)	(120.82, −5.63)	(150.51, −11.78)	(179.96, −17.81)	(209.25, −23.77)
$\rho = 1.1$, $\delta = 12°$	(82.44, 1.01)	(110.38, −5.63)	(137.90, −12.37)	(165.20, −18.80)	(192.38, −25.16)
$\rho = 1.1$, $\delta = 15°$	(75.52, 1.24)	(101.49, −5.93)	(127.11, −12.84)	(152.53, −19.61)	(177.84, −26.31)
$\rho = 1.1$, $\delta = 18°$	(69.61, 1.44)	(93.83, −6.02)	(117.76, −13.22)	(141.51, −20.29)	(165.17, −27.27)
$\rho = 1.1$, $\delta = 21°$	(64.48, 1.62)	(87.15, −6.09)	(109.56, −13.54)	(131.83, −20.85)	(154.02, −28.08)
$\rho = 1.1$, $\delta = 24°$	(59.99, 1.79)	(81.26, −6.13)	(102.32, −13.80)	(123.25, −21.33)	(144.10, −28.78)
$\rho = 1.1$, $\delta = 27°$	(56.02, 1.94)	(76.03, −6.16)	(95.86, −14.02)	(115.57, −21.74)	(135.23, −29.39)
$\rho = 1.1$, $\delta = 30°$	(52.48, 2.07)	(71.34, −6.19)	(90.05, −14.21)	(108.67, −22.10)	(127.23, −29.92)

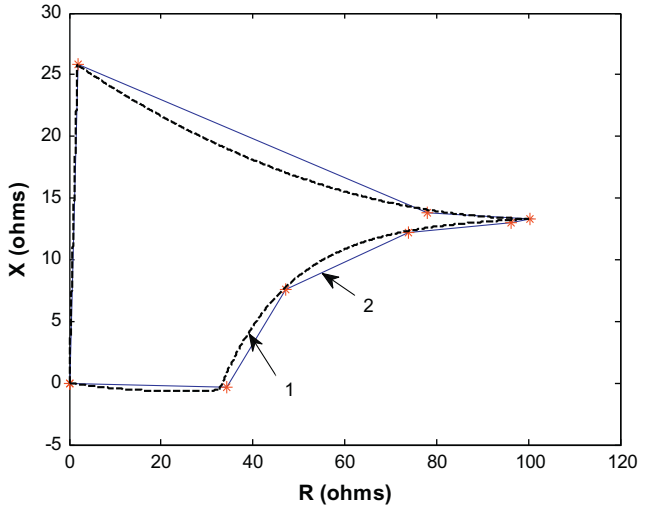

Fig. 11. (1) Ideal trip characteristic and (2) approximate characteristic obtained from neural networks output.

Table 3
Value of seen impedance in relay point for different position of fault on-line length and $R_F = 10\ \Omega$.

L = 30%	L = 50%	L = 70%	L = 90%	L = 98%
11.71 + j	15.83 + j	23.66 + j	56.33 + j	82.45 + j
7.095	11.78	15.51	15.32	14.4

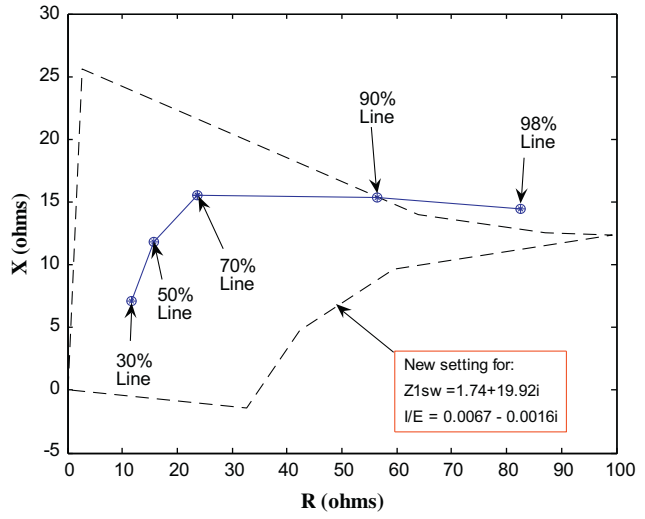

Fig. 12. Seen impedances from relay point for faults occurred in different points of transmission line and $Z_{1SW} = 20\angle 85°$, $I_{WP}/E_{AW} = 0.0067 - j\ 0.0016$.

Therefore:

$$W_{21}X_A(a) + W_{22}R_A(a) + W_{20} = 0$$
$$W_{21}X_A(b) + W_{22}R_A(b) + W_{20} = 0 \quad (10)$$

and supposing that the linear output is required to be positive on the trip region side and selecting $W_{21} = -1$, the weights are given by:

$$W_{21} = -1$$
$$W_{22} = (X_A(b) - X_A(a))/(R_A(b) - R_A(a)) \quad (11)$$
$$W_{20} = X_A(b) - R_A(b)(X_A(b) - X_A(a))/(R_A(b) - R_A(a))$$

Table 4
Value of seen impedance in relay point for different fault resistance occurred in 60% of line length.

$R_F = 10\ \Omega$	$R_F = 20\ \Omega$	$R_F = 30\ \Omega$	$R_F = 40\ \Omega$	$R_F = 50\ \Omega$	$R_F = 60\ \Omega$	$R_F = 70\ \Omega$
18.99 + j	32.48 + j	43.31 + j	52.17 + j	59.56 + j	65.80 + j	71.15 + j
18.83	11.9	10.73	10.02	9.59	9.36	9.24

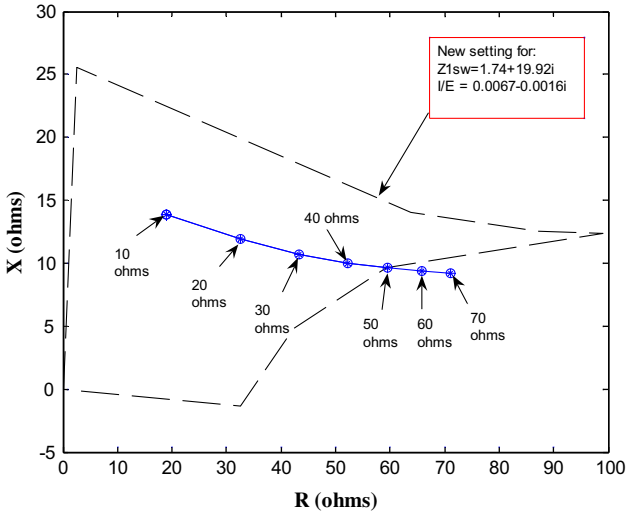

Fig. 13. Seen impedances from relay point for faults occurred in 60% of line length and different fault resistances ($Z_{1SW} = 20\angle 85°$, $I_{WP}/E_{AW} = 0.0067 - j\ 0.0016$).

Table 5
The weight values comparable with trip characteristic presented in Fig. 3.

i	W_{i0}	W_{i1}	W_{i2}
1	0	1	−9.909
2	26.049	−1	−0.186
3	0	1	−0.219
4	18.083	−1	−0.064
5	0	1	−0.144
6	13.667	−1	−0.013
7	0	1	−0.125
8	5.501	−1	0.069
9	0	1	−0.162
10	−7.178	−1	0.283
11	0	1	−0.113
12	−22.187	−1	0.638
13	0	1	0.043

During fault, after fault detection and fault classification, a digital distance relay calculates the apparent reactance and resistance.

From these apparent values the linear outputs L1–L13 can be obtained. In proposed adaptive scheme, the logical values comparable with positive or negative value of these outputs using "AND" and "OR" operations between them are used to reach a final trip decision as shown in Fig. 7.

It is obvious that the computational task for the processor is small. In this study case, the post-fault online calculations are no more than 13 multiplication, 19 additions and 12 logic operations. This involves relatively little real time digital processing and can be well done by 16-bit microprocessors [6].

Evidently, the resistance and reactance values of points "a" through "g", all depends on Z_{1SW} and I_{WP}/E_{AW}. Therefore, to obtain them, seven FFB[1] neural networks are used here. The inputs of each

[1] Feed Forward Back propagation.

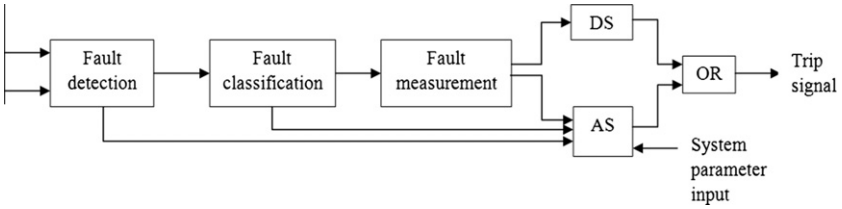

Fig. 14. Block diagram of distance relay with the adaptive setting scheme [6].

of them are Z_{1SW} and I_{WP}/E_{AW} and the outputs are resistance and reactance of one of the points "a" through "g". The number of inputs and outputs of each network are 2. If other trip characteristic were used for distance relay, the required number of outputs might be less or more than this case. In fact, the number of network outputs will be depended on the number of variables required to determine relay trip region. The reason that we used seven networks with two outputs instead one network with 14 outputs, is to increase their reliability and learning speed and to decrease their total error.

To train the networks, for each point, 150 cases are acquired by changing in parameters which expressed above. The resistance and reactance value of each point is acquired by changing in R_F and fault location as shown in Fig. 8.

To define and train each network, we used MATLAB neural network toolbox. The kind of networks is perceptron and they were trained by back-propagation method. The neural transfer function of input layer is tangent sigmoid and of output layer is linear. Usually, the number of input layer neurons is determined according to performance function of network and experimentally. For example, here, this number is considered 150 for 3rd network. Training function is "scaled conjugate gradient back propagation".[2]

The diagram of 3rd neural network is shown in Fig. 9. This network was trained using values presented in Table 2 and obtained from relation 4. Its performance function curve is shown in Fig. 10.

4. Testing of proposed scheme and results

Since Z_{1SW} and I_{WP}/E_{AW} have various values, trained networks must be tested to ensure from their proper performance. For example, suppose that Z_{1SW} and I_{WP}/E_{AW} is equal to $20\angle 85^\circ$ and $0.0067 - j\,0.0016$ respectively. Entering these values to neural networks program, the points "a" through "g" will be acquired.

The ideal trip region and the characteristic formed by outputs of networks, has been shown in Fig. 11. It is evident from this figure that approximately all of the output points of networks (specified with stars) are located on ideal trip characteristics. This subject approves that neural networks have very good accuracy.

To test the performance of this adaptive unit, computer simulation for a fault located on 90% of line length has been done. Basically, the measured impedance in relay point must be positioned inside of the trip characteristic. For longer distances the impedance must be positioned outside of that region. Table 3 shows the fault location and seen impedance value in relay point. The fault resistance has been considered equal to 10 Ω.

In Fig. 12, the adaptive trip characteristic and the location of impedances of Table 3 have been shown, and the relay performance can be discovered from this figure. As it is obvious from Fig. 12, for a fault located on distances shorter than 90% of line length, the proposed adaptive unit will detect it properly and it will not render trip command for longer distances.

Now, for the same values of Z_{1SW} and I_{WP}/E_{AW}, we change the fault resistance and measure impedance in relay point. The fault is positioned on 60% of line length. Table 4 represents the measured impedance values.

It can be seen easily from Fig. 13 that increasing fault resistance, the locus of seen impedance do not track complete horizontal direction and the measured impedance drop inside of trip characteristic for the faults up to 50 Ω. This adaptive method, improves the protection system treatment against fault resistance variation because a polygonal characteristic treatment is better than mho characteristic against fault resistance variations.

Now, it is the time that the presented weights in previous section for lines L1–L13 have to be obtained from neural networks output points. The results can be observed in Table 5.

After the weights and positive or negative value of linear outputs for online seen impedance was calculated, the adaptive unit obtains a trip decision.

Extra high speed digital distance relays have been implemented with different algorithms and some can operate within one cycle or even a few milliseconds of fault occurrence. A typical digital distance relay consists of a fault detection unit, a fault classification unit, a fault measurement unit and a trip region comparison unit. A disturbance or a fault is first detected and then the fault type is determined. Apparent reactance and resistance are calculated in the measurement unit. Generally, successive estimates of the impedance are compared with the boundary conditions at every sampling interval. To improve the performance of currently available digital distance relays a practical scheme shown in Fig. 14 was designed.

In the block diagram, an adaptive setting (AS) unit works in collaboration with a default setting (DS) unit and the default setting unit with a preset conventional quadrilateral characteristic remains valid during a fault until its recovery. The adaptive setting (AS) will be unblocked for a certain period during a fault only. One reason for this is that the accuracy of the measured impedance is adversely affected by transient components in the first cycle of a fault and using the adaptive setting with an almost whole line boundary may cause mal-operation. Another reason is that false tripping may also be caused by the removal of the remote-end infeed.

5. Conclusion

Power output of a wind farm fluctuates throughout a day and the transmission system connecting such a farm to the grid, will be exposed to these power variations. The simulation results for a two-terminal line which connects the wind farm to the grid, show that the wind farm conditions, including the number of generating units and the ratio of local current and voltage affect the trip boundary of the distance significantly. To take into account the changing wind farm condition, an adaptive setting method for different zones of distance is proposed. In method discussed in this paper, a separate adaptive unit that works in collaboration with a default setting unit and uses local information of wind farm has been used and the output points of some neural networks, construct the characteristic of this unit. Using of neural network in adaptive setting has a good accuracy, reliability and also high

[2] TRAINSCG.

speed because the number of online measurements is limited in it and the need of large amount computer memory has been solved. The proposed adaptive scheme in this paper does make a digital distance relay operates with improved sensitivity, selectivity and speed.

References

[1] Erikson PB et al. System operation with high wind generation. IEEE Power Energy Mag 2005;3(6):65–74.
[2] Jang SI, Choi JH, Kim JW, Choi DM. An adaptive relaying for the protection of a wind farm interconnected with distribution network. In: Proc IEEE PES trans dis conf expo, vol. 1; 2003. p. 296–302.
[3] Brahma SM, Girgis AA. Development of adaptive protection schemes for distribution systems with high penetration of distribution generation. IEEE Trans Power Del 2004;19:56–63.
[4] Hornak D, Chau NHJ. Green power-wind generated protection and control consideration. In: Proc IEEE 57th annu conf protective relay eng; 2004. p. 110–31.
[5] IEEE Guide for protective relay applications to transmission lines. standard C37.113-1999, February 29, 2000.
[6] Xia YQ, Li KK, David AK. Adaptive relay setting for standalone digital distance protection. IEEE Trans Power Del 1994;9:480–91.
[7] Moore PJ, Aggarwal RK, Jiang H, Johns AT. New approach to distance protection for resistive double-phase to earth faults using adaptive techniques. IEEE Proc Gen Trans Distrib 1994;141(4):369–76.
[8] Li KK, Lai LL, David AK. Stand alone intelligent digital distance relay. IEEE Trans Power Del 2000;15:137–42.
[9] Sidhu TS, Baltazar DS, Palomino RM, Sachdev MS. A new approach for calculating zone-2 setting of distance relays and its use in an adaptive protection system. IEEE Trans Power Del 2004;19:70–7.
[10] Orduna E, Garces F, Handschin E. Algorithmic-knowledge-based adaptive coordination in transmission protection. IEEE Trans Power Del 2003;18:61–5.
[11] Izykowski J, Rosolowski E, Saha M. Adaptive digital distance algorithm for parallel transmission lines. In: Proc IEEE PowerTech conf, vol. 2; 2003.
[12] Jonsson M, Daalder JE. An adaptive scheme to prevent undesirable distance protection operation during voltage instability. IEEE Trans Power Del 2003;18:1174–80.
[13] Dutra R, Fabiano L, Oliveira W, Saha MM, Lindstorm S. Adaptive distance protection for series compensated transmission line. In: IEEE/PES trans distrib conf expo; 2004. p. 581–6.
[14] Pradhan AK, Joos G. Adaptive distance relay setting for lines connecting wind farms. IEEE Trans Energy Conv 2007;22:206–13.